# Chemical wear of carbon and silicon carbide-based refractory materials by silicomanganese metal

**Wesley Banda – Mintek, South Africa**
**[1]Joalet Steenkamp and [2]Elias Matinde**
**– [1]Mintek, [2]University of Witwatersrand, South Africa**

*Carbon and silicon carbide-based refractory materials are refractory materials commonly applied in submerged arc furnaces producing silicomanganese. Recent studies on refractory wear in industrial-scale furnaces identified two high-wear areas, namely, the furnace tap-hole and the furnace hearth. Laboratory-scale investigations offer an opportunity to study in detail the mechanisms responsible for wear. In particular, the rotating finger experiment allows for the study of both chemical and mechanical wear mechanisms. The paper proposes a design for the rotating finger experimental setup, and reports on the sourcing, preparation and characterisation of materials to be applied in the experiments. Thermodynamic calculations allow for the theoretical study of the effects of changes in process variables, namely temperature and Si-content, on refractory wear. FactSage™ software was applied to quantify the potential for refractory wear by chemical reaction with, and/or dissolution into, the silicomanganese metal. Temperature was varied between 1550°C, 1600°C and 1650°C, and Si content between 16 wt. %, 17 wt. % and 18 wt. %. From the FactSage™ calculations, maximum dissolution is expected to occur at 1650°C, with 1.4 wt. % decrease for carbon-based refractory and 2.9 wt. % decrease for silicon carbide-based refractory. The decrease in weight is due to dissolution only, as no reaction products were predicted to form. Increasing the Si-content of the metal from 14.9 wt. % to 18 wt. % resulted in an increase in the dissolution rate of both types of refractory materials, as well as formation of silicon carbide reaction product in the carbon-based refractory.*

**KEYWORDS:** *SILICOMANGANESE – FACTSAGE™– ROTATING FINGER TECHNIQUE – HEARTH –* REFRACTORY *WEAR*

## INTRODUCTION

Silicomanganese (SiMn) typically contains 65 – 68 % Mn, 12.5 – 21 % Si, 1.5 – 3.0 % C, 0.2 % P, and 0.04% S [1]. SiMn is produced commercially in three-phase, alternating current (AC), submerged arc furnaces (SAF) [2-3].

Fig.1 shows a typical refractory design installed in an air-cooled steel shell, consisting of an insulating back lining, a carbon-based working lining, and a silicon-carbide (SiC) tap block creating a single level tap-hole through which both metal and slag are tapped. The insulating back lining consists of super-duty fire-clay bricks, typically consisting of 53.6% $SiO_2$, 42.0% $Al_2O_3$, 1.5% $Fe_2O_3$, 1.6% $TiO_2$, 0.15% CaO, and 0.3% MgO. The working lining consists of a cold-rammed high-grade carbon material typically consisting of 50 – 70% anthracite, 15 – 25% graphite, 6 – 12% resin, 2 – 7% tar, 1 – 5% clay, and 1 – 5% $Al_2O_3$. The tap block was built using SiC bricks, typically consisting of 75% SiC, 23.4% $Si_3N_4$, 0.3% $Fe_2O_3$, 0.3% $Al_2O_3$, and 0.2% CaO. Alternative tap block materials available include carbon-based cold ramming paste (similar to the material installed as working lining) and premanufactured carbon blocks [4], [5]. On a dry basis, the carbon-based cold ramming paste typically contains 6.3% ash, 1% volatile matter, and 92.6% carbon. On the other hand, the carbon block contains 22.7% ash, 0.2% volatile matter, and 77.0% carbon. Both materials typically contain about 0.1% moisture on an air-dried basis.

For the 48 MVA SAF excavated in South Africa in 2013, two high wear areas existed as indicated in Fig. 1:

INDEX

The tap-hole refractory, and the hearth refractory [6-8].

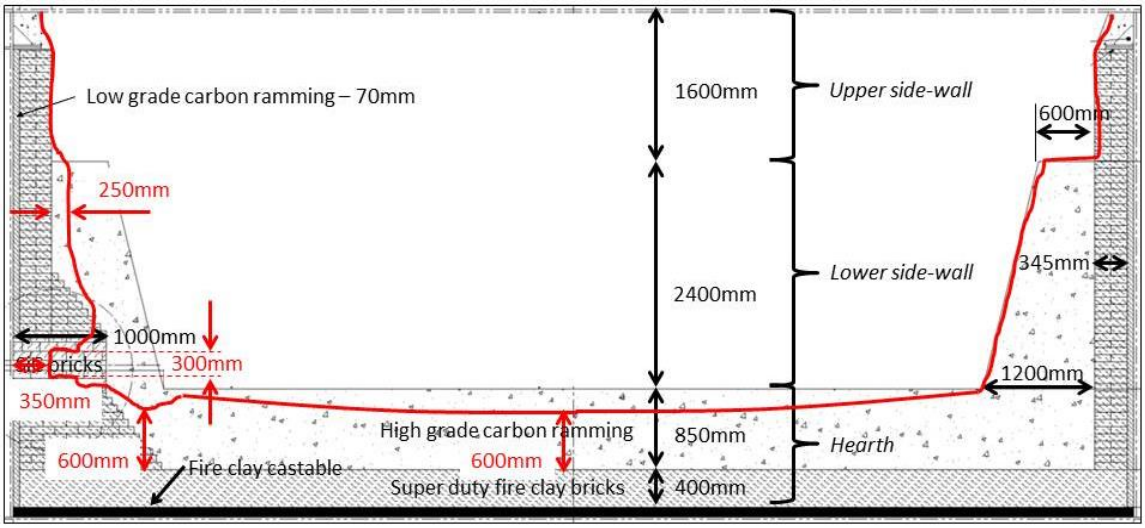


***Fig. 1**: Refractory wear profile (red line) of a 48 MVA SAF, used for SiMn production, excavated in 2013 in South Africa superimposed onto the refractory design drawing (black drawing).*

In a study [9] to characterize the chemical wear of two carbon-based refractory materials in the form of carbon block and carbon ramming paste in a SiMn furnace tap-hole, the complex reactions between process materials such as metal and slag, with the carbon-based refractory materials were studied in order to improve the understanding of the potential of chemical wear of the refractory material, when tapping both the alloy and slag through a single-level tap-hole. It was determined experimentally that silicon carbide (SiC) and metal containing silicon and manganese were formed as products of the reaction between the slag and refractory material, thereby contributing to the chemical wear of the carbon-based refractory material [9].

Subsequent thermodynamic calculations, were done based on tapped metal composition data collected over three months, from seven industrial plants in South Africa. The calculations indicated the potential for metal and refractory interaction being a further source of wear, in both the tap-hole and hearth refractory [10-11]. Depending on the process temperatures, refractory wear by dissolution as well as chemical reaction forming SiC were identified as two potential wear mechanisms in the case of carbon-based refractory materials. SiC-based refractory materials were considered as an alternative, but these could also be prone to dissolution depending on the process temperature.

Based on these findings, the need for further investigation into the wear of carbon-based refractory material by SiMn alloy at laboratory scale was identified. The objective of the study is to investigate the differences in wear rates between two types of prebaked ramming paste materials, one carbon-based (type K) the other SiC-based (type SiC), in silicomanganese metal using the rotating finger experimental setup. The experiments will simulate the wear mechanism in both the tap-hole and the hearth of SAFs used in the production of SiMn. The project focuses on the development and testing of a method to measure mechanical and chemical wear of the carbon based refractory at different temperatures and alloy composition under inert furnace atmosphere conditions. Initial work consisting of material sourcing, preparation, and characterization, as well as thermodynamic calculations to predict the wear expected, is reported here. In addition, the experimental design currently being developed for the rotating finger experiments is discussed as background.

# BACKGROUND

Fig. 2 shows the design of the rotating finger experimental set-up to be applied in the study. A refractory cylinder with a diameter of 50 mm and height of 55 mm is attached to a cylindrical graphite rod with a height

INDEX

of 550 mm and diameter of 20 mm. The rod is attached to the cylinder using graphite glue. The rod and cylinder assembly is then mounted onto an extension arm, which is connected to an electric rotating motor. A graphite crucible with an outer diameter of 200 mm and height of 250 mm is placed inside the induction furnace to facilitate heat transfer, and alumina bubbles are added between the graphite crucible and induction furnace chamber to achieve the height specified in Fig. 2, so that the graphite crucible is within the range of the induction coils, for maximum heat transfer. In addition, an alumina crucible with an outer diameter of 100 mm and height of 115 mm is placed inside the graphite crucible with alumina bubbles to get the height inside the graphite crucible as specified in Fig. 2. The SiMn alloy and refractory cylinder will then interact inside the alumina crucible, simulating conditions inside the furnace. B-type thermocouples are used to measure the temperatures inside the induction furnace, and an oxygen probe is used to measure the oxygen partial pressure inside the reaction chamber.

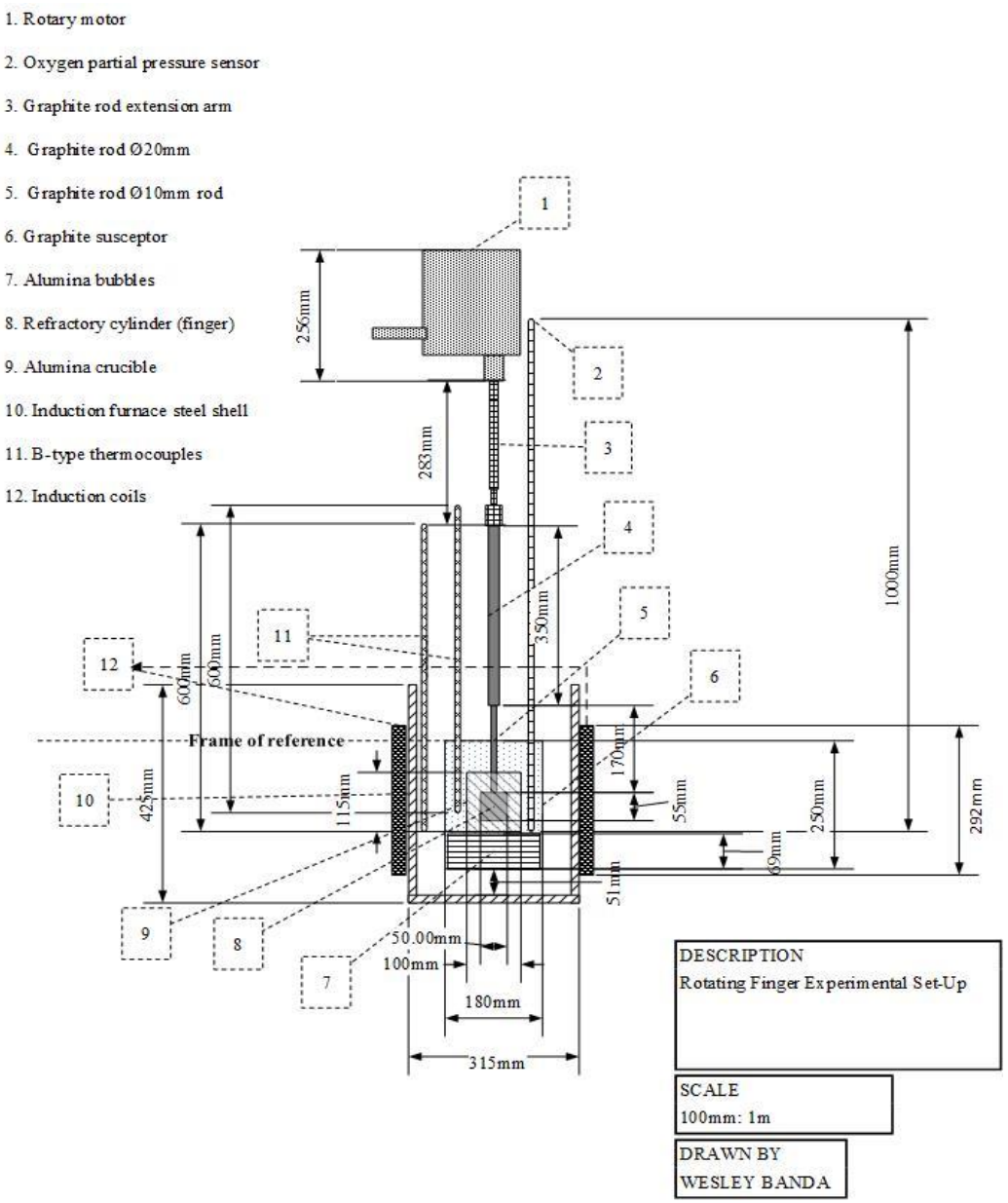


**Fig. 2:** Rotating finger experimental set up

The variables involved in the experiments are temperature, alloy Si content, motor speed, reaction time, heating rate, and furnace atmosphere. The fixed variables include the heating rate, which will be manually

adjusted at increments of 0.5 amps every 30 minutes, and reaction chamber atmosphere (argon). The controlled variables are listed below. When the influence of a specific variable on refractory wear is evaluated, all other variables will be fixed at the baseline value.

1. Temperature will be varied between 1550 and 1650°C, at 50°C intervals. The baseline value for temperature is 1600°C. These values represent the typical temperatures for the SiMn producing furnaces, thus they were chosen to represent their operation conditions.
2. Si content of the alloy will be varied between 14 wt. % and 18 wt. %, at 1 wt. % intervals. The baseline value for Si content of the alloy will be 14.7%. The SiMn composition of the alloy (14.7 wt. %) was below grade B, which is normally produced by Transalloys, thus the values chosen cover the composition of the as received alloy, as well as those specified by the ASTM standard for grade B [12]
3. The reaction time will be varied between 60 and 120 minutes at 30 minute intervals. The baseline value for reaction time will be 90 minutes. The baseline operating time used for laboratory induction furnace is 90 minutes. This time period will then be varied by starting off at 60 minutes, all the way up to 120 minutes.
4. The motor speed will be varied between 0 (static) and 100 rpm, at 50 rpm intervals, allowing the measurement of the mechanical wear effects. The midpoint, 50 rpm, will be used as the baseline.

# METHOD

## *MATERIAL SOURCING AND PREPARATION*

Industrial SiMn metal samples were obtained from Transalloys, one of the two producers of SiMn in South Africa [3]. Refractory samples were obtained from Elkem Carbon, a Norwegian-based international supplier of carbon-based refractory materials [13].

At Transalloys, the alloy is tapped into ladles and then layer-cast as layers in alloy beds. Once cooled, the alloy is collected by front-end loader and taken to the alloy handling plant. The sample used in the present experiments was collected by hand from the alloy bed. Fig. 3 shows the sample preparation flow sheet. The as-received alloy was first weighed, crushed and milled to -200 µm. The sample was weighed and split into two. One split was weighed and further split into 20 samples using a 20-cup rotary splitter. Samples 1 and 2 were used for characterisation, samples 3 to 11 will be used for refractory tests with the type K refractory, and samples 12 to 20 will be used for refractory tests with the type SiC refractory.

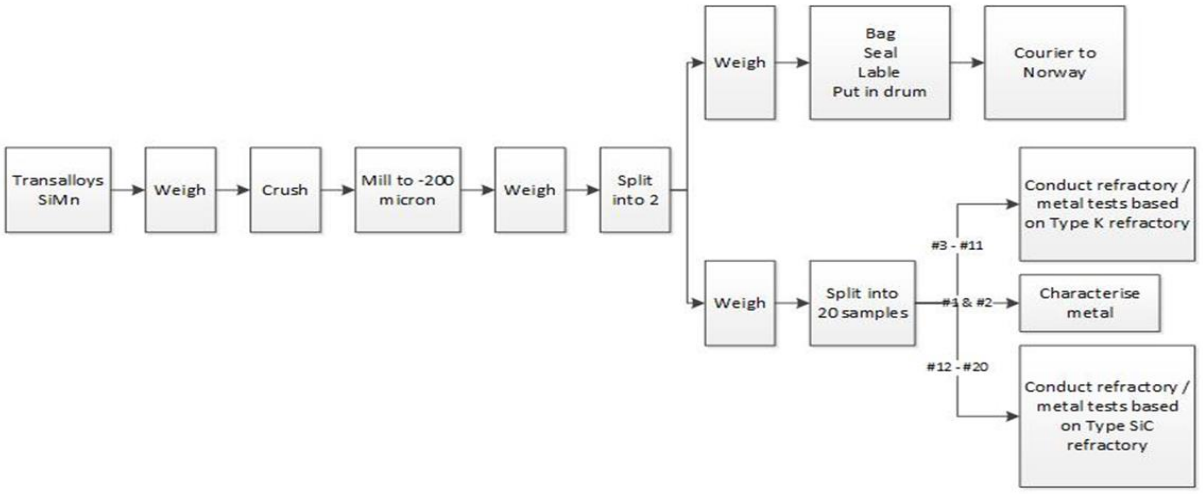


**Fig. 3**: SiMn sample preparation flowsheet

INDEX

The refractory samples were prepared by Elkem Carbon at their research facilities in Kristiansand, Sweden. Two types of refractory materials were used: (1) Type K, typically consisting of 80-90% electrically calcined anthracite, 10-20% coal tar pitch and 5% ash content [14], and (2) Type SiC, typically containing 60-80% silicon carbide, 10-20% silicon metal and 10-20% coal tar [15]. The refractory paste was rammed in a Fisher sand rammer test machine. The sand rammer is made up of a frame, pendulum and pusher arm weight – this equipment is used for testing strength of molding sand. The samples were prepared as a larger sample by the sand rammer and as the machine rammed the samples, the density of the sample was measured as a function of each stroke. For curing and baking the samples, the rammed samples were placed inside a high-temperature steel box with coke on all sides to form a coke bed and to reduce oxidation from surrounding air. The samples were heat treated by increasing the temperature at a rate of 20°C/hour to 950°C, where they were held for 1 hour inside a muffle furnace. In order to cool the samples, the temperature was reduced from 950°C to 30°C over approximately 20 hours. Cylindrical refractory samples 50 mm in diameter and 55 mm height were then core-drilled from the larger sample. The 10mm diameter holes for attachment of the graphite rod were drilled out afterwards on individual sample cylinders.

Testing of refractory materials is generally done by evaluating three aspects: characterization or data sheet properties, service-related properties, and design-related properties [16]. The rotating finger experiment discussed above aims to characterize service-related properties. In the next section, data sheet properties are addressed, which include the chemical composition, bulk density, and apparent porosity, as well as mineral composition. The chemical composition of the as-received SiMn alloy was determined as well.

## *MATERIAL CHARACTERIZATION*

The bulk chemical composition of three representative SiMn samples was determined by wet chemistry and X-ray fluorescence (XRF). The carbon composition in the alloy was determined using ultimate-analysis-by-LECO methods.

Chemical analysis of the refractory material was performed to evaluate the concentrations of the elements present. The bulk chemical analyses evaluated include, proximate [17], ultimate and ash analyses [18].

Proximate analysis [17] was used for the refractory samples and measured the moisture, ash and volatile matter content . The fixed carbon was calculated by difference. Moisture content [19] of a sample was determined using a drying oven, where the moisture of the sample was obtained by difference of the sample masses before and after drying. A thermo-gravimetric analyzer (TGA) was used to obtain the volatile matter content and ash content by temperature variations that result in mass changes within the sample as the atmosphere changes from inert to oxidizing. The fixed carbon was determined by difference.

Ultimate analysis was done to obtain elemental analyses of the carbon-based refractory materials. The results from the ultimate analysis were used to determine the elemental composition of the refractory including carbon, hydrogen, nitrogen, and sulfur. Oxygen was determined by difference [20].

The bulk phase chemical analysis was done using X-ray diffraction (XRD) methods, which provided means of quantifying and characterizing different crystalline phases as well as the amorphous phases present. A Bruker D8 diffractometer with an acceleration voltage of 35kV and cobalt tube with Fe-low beta filter was used, with the 2θ angle ranging from 2 to 80 degrees and step size of 0.02° 2θ.

Microscopic examination of the refractory was done using a Zeiss Evo MA15, which allowed the identification of the specific phase chemistry of the different phases present in the refractory, characterized via scanning electron microscope-energy dispersive spectroscopy (SEM-EDS) using an acceleration voltage of 20 kV, and electron microprobe analysis (EMPA) using an acceleration voltage of 15 kV. Backscattered electron images (BSE) from the SEM analysis display compositional contrast that result from different atomic number elements and their distribution. EDS allowed particular elements to be identified together with their relative

compositions [21]. A Cameca SX50 Electron Probe Microanalyser (EMPA) provided quantitative analysis of the material with reference to a standard. In an EMPA a beam of electrons is focused on a specific point, resulting in emission of X-rays of wavelength characteristic of the element present [22]. The beam was generated at 20 kV with a probe current of 30 nA and a spot size of 5 µm. EMPA analysis provided a graph with the distribution of the elements. Backscattered electron images were also produced, which can be used to identify different chemical phases [22].

The bulk density of a porous material is the ratio of its mass to its bulk volume [16], and was calculated using Equation 1. The apparent porosity is the ratio of the open pores in the material to the bulk volume, and was calculated using Equation 2. The Archimedean evacuation method was used to measure both the bulk density and apparent porosity. A method based on an ASTM standard C20-00 was developed by Mushwana and Steenkamp [23] which was then used as the standard procedure to do the measurements.

$$\rho = [D/(D - S)(\rho_o - \rho_L)] + \rho_L \quad (1)$$

Where:
$\rho$ = Bulk density of the sample (g/cm$^3$)
$\rho_o$ = Density of auxiliary liquid (g/cm$^3$)
$\rho_L$ = Density of air (taken as 0.0012 g/cm$^3$)

$$P = [(W - D)/V]*100 \quad (2)$$

Where,
P = Apparent porosity (%)
W = Saturated weight (g)
D = Dry mass (g)
V = Exterior volume (cm$^3$), based on *Equation 3*

$$V = W – S \quad (3)$$

Where,
S = Suspended weight (g)

## *THERMODYNAMIC CALCULATIONS*

The Equilibrium model in FactSage™ 6.4 [24] was applied in the thermodynamic calculations. The dataset developed by Tang and Olsen [25] for ferromanganese was used together with the FactPS database for pure substances. The SiMn metal analysis reported in the background section was used as basis for the thermodynamic calculations to predict the potential wear of the SiC and the carbon refractory. Variables tested were temperature and Si composition in the metal. The temperatures were selected to simulate the typical operating temperatures for SiMn producing furnaces, and were varied from 1550°C to 1650°C, with the midpoint temperature of 1600°C being chosen as the baseline temperature. SiMn composition was varied at 16 wt. %, 17 wt. % and 18 wt. % silicon. Since Transalloys normally produces grade B SiMn, the modelling was done based on the grade B specification.

# RESULTS AND DISCUSSION

## *MATERIAL CHARACTERIZATION*

The bulk chemical composition of the SiMn alloy is reported in Tab. 1. The mineralogical analysis of the SiMn alloy indicated that there were two phases present as seen Fig. 4, where the two phases can be distinguished by a light grey area (A) and a dark grey area (B). SEM-EDS and EMPA results in Tab. 1

indicate that phase A is a high Mn and low silicon phase, while phase B is a high silicon phase with lower Mn levels relative to phase A. The presence of carbon was also identified in phase A. The standard specification for SiMn alloy in ASTM-A483 [12] indicates that grade B composition for Mn is in the range of 65-68 wt. % and Si is in the range of 16-18.5 wt. %. Thus from the chemical analyses, the SiMn alloy can be considered grade C as the Si composition falls within the range of 12.5-16 wt. %.

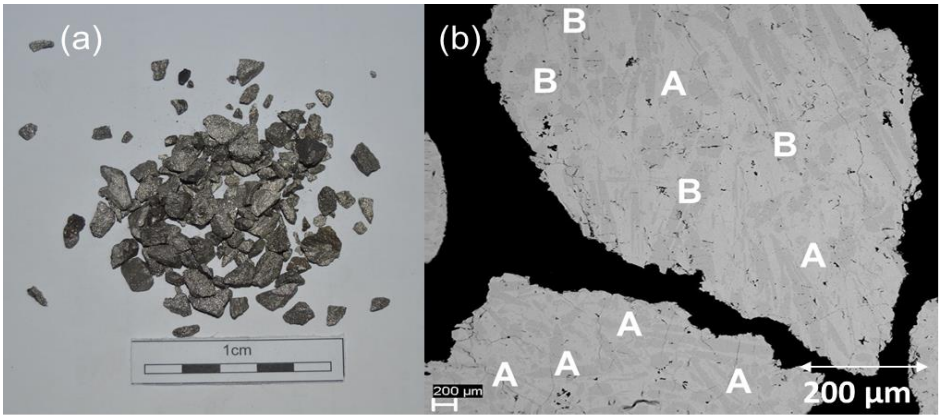


***Fig. 4**: SiMn alloy (a) photograph of as-received material and (b) SEM BSE image Images measured at 20 kV acceleration voltage. Scale bar indicates 200 µm.*

***Tab. 1**: Composition of two silicomanganese alloy phases, present in as-received industrial samples, identified by SEM in Fig 2.. The calculated average composition was determined by normalised EDS analysis at 20 kV acceleration voltage, with standard deviations indicated in brackets. EMPA, was done on randomly selected grains at 15 kV and 20 nA,and spot size 5µm. Normalized SiMn alloy XRF and Wet chemistry analysis are also included*

| Area | | C | Si | Mn | Fe | Total |
|---|---|---|---|---|---|---|
| A | SEM-EDS | | 9.3 (1.7) | 75.3 (5.0) | 15.5 (3.4) | 100.0 |
| | EMPA | 2.4 (0.2) | 9.7 (0.2) | 73.9 (1.3) | 14.0 (0.8) | 100.0 |
| B | SEM-EDS | | 20.4 (0.4) | 65.6 (1.0) | 14.0 (0.6) | 100.0 |
| | EMPA | - | 23.1 (0.2) | 62.9 (0.9) | 14.9 (0.9) | 100.0 |
| Bulk sample | Wet chemistry | 1.7 (0.0)* | 14.7 (0.4) | 67.3 (0.1) | 16.3 (0.1) | 100.0 |
| | XRF | 1.7 (0.0)* | 15.3 (0.1) | 67.5 (0.2) | 15.5 (0.1) | 100.0 |

**Carbon analysis was done using the LECO*

In Fig. 5 (b) the type K refractory SEM-BSE image can be seen to have a major carbon phase and minor intrusions of SiC which may have resulted from surface contamination. In Fig 5 (d) the SiC SEM-BSE image can be seen to have the SiC as the major phase, with silicon oxide and silicon present as the minor phases. Proximate analysis in Tab. 2 is in line with the SEM-BSE observation, where the type K has a major C composition of 86.4 wt. % and the minor SiC reported to the ash which has a composition of 10.9 wt. % C. This is comparable with the data sheet information supplied for the type K [14], where the C is within the 80-90% composition range of electrically calcined anthracite. The ash content from the proximate analysis, in comparison to the data sheet information supplied for the type K [14], is slightly higher by 5.9 wt.%. The SiC type has a major ash composition of 95.9 wt. %, which is within the range to the type SiC data sheet information [15] where a total summed composition range of 70-100% would be for both SiC and Si, and both would then report to the ash. The minor carbon composition of 1.6 wt. % for the type SiC was below the 10-20% range given for the coal tar pitch in the data sheet [15]. Tab. 3 contains the the ultimate analysis of

INDEX

the refractory materials, and the results also are in line with the SEM-BSE image, where the type K refractory has more fixed carbon than the type SiC.

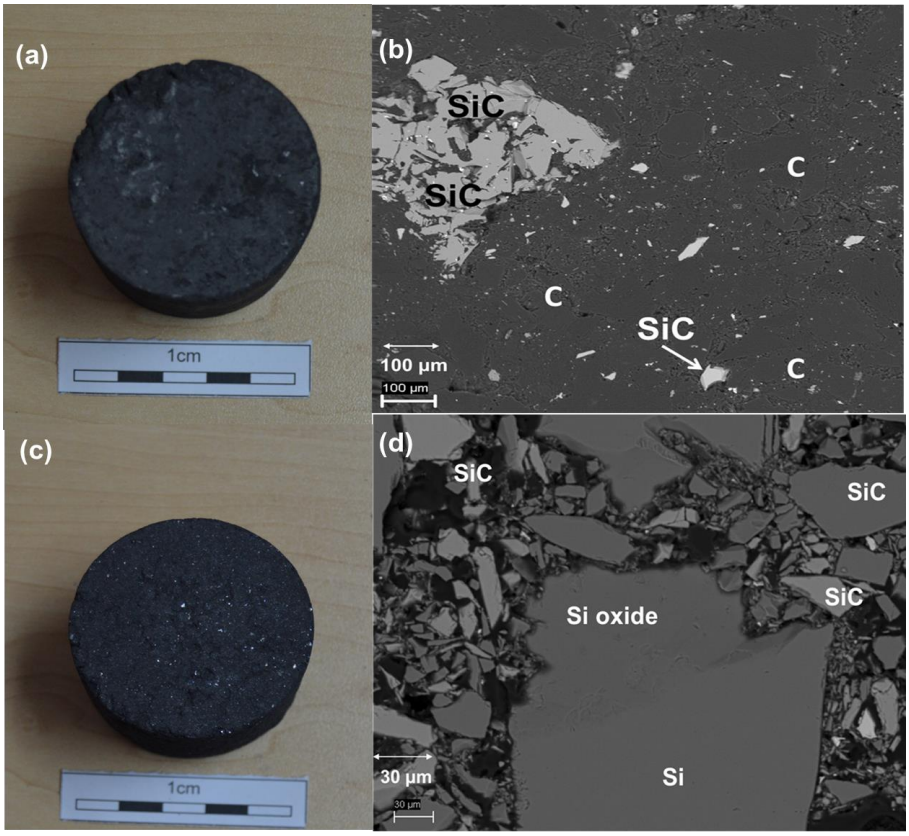


***Fig. 5**: (a) Type K refractory cylinder as received from Elkem, (b) Type K Refractory SEM image measured at 20 kV acceleration voltage. Scale bar indicates 100 µm. (c) Type SiC refractory cylinder as received from Elkem and (d) SiC-type Refractory SEM image measured at 20 kV acceleration voltage. Scale bar indicates 30 µm.*

***Tab. 2**: Proximate analysis of of the type K and type SiC refractory as received from Elkem. The table contains average values of triplicated results and the standard deviation is indicated in brackets. ASTM-D3172, ASTM-D3173, ASTM-D3174,* [17]–[19] *were used as a standard procedures for the proximate analysis.*

| | Ash | Fixed Carbon | Moisture | Volatile | Total |
|---|---|---|---|---|---|
| Type K Refractory | 10.9 (7.3) | 86.4 (9.9) | 0.3 (0.1) | 2.4 (2.5) | 100.0 |
| Type SiC Refractory | 95.9 (1.0) | 1.6 (2.7) | 0.4 (0.0) | 2.4 (1.8) | 100.2 |

***Tab. 3:** Ultimate analysis of the type K and type SiC refractory as received from Elkem. The table contains average values of triplicated results and the standard deviation is indicated in brackets.*

| | Hydrogen | Nitrogen | Oxygen | Carbon | Sulphur | Total |
|---|---|---|---|---|---|---|
| Type K Refractory | 0.6 (0.3) | 0.4 (0.1) | 4.7 (7.6) | 96.7 (1.0) | 0.1 (0.0) | 102.5 |
| Type SiC Refractory | 0.2 (0.0) | 0.2 (0.0) | 0.0 (0.0) | 30.7 (0.8) | 0.0 (0.0) | 31.1 |

INDEX

Density and porosity measurement results for the two refractory samples are presented in Tab. 4. The average measured density values are in line with the values supplied by the manufacturer data sheet [14-15]. The calculated porosity value for the type K refractory is also comparable to that given by the data sheet. Comparing the bulk densities of the two refractory materials, it can also be seen that for a given volume, SiC type refractory will have a larger mass than the type K refractory.

***Tab. 4**: Density and Porosity Measurement results. The standard deviation for the average measured densities are given in brackets*

| | Density (kg/m3) | | | Porosity (%) | |
|---|---|---|---|---|---|
| | Average measured density | Calculated bulk density | Manufacturer data sheet | Calculated porosity | Manufacturer data sheet |
| *type K Refractory* | *1480 (0.002)* | *1818* | *1460* | *18* | *19* |
| *type SiC Refractory* | *2324 (0.007)* | *3000* | *2300* | *23* | *Not supplied* |

## *THERMODYNAMIC CALCULATIONS*

The following section contains the results of the FactSage™ calculations for the type K and type SiC refractory materials. In Tab. 5 temperature was varied while keeping other variables constant, i.e. Si wt. % in the alloy is held constant at 14.74. Tab. 5 contains the FactSage™ modelling results, where both refractories show an increase in dissolution into the metal with an increase in temperature. The type K refractory lost 1.4 g due to dissolution into the SiMn metal at 1650ºC, and the type SiC refractory having the highest mass lost due to dissolution of about 2.9 g at the same temperature. The wear is completely due to a dissolution mechanism and not a reaction, as no other products were formed.

***Tab. 5**: Refractory dissolution with temperature variations*

| Refractory type | Initial mass (g) | Mass (g) (T =1550 C) | Mass (g) (T =1600 C) | Mass (g) (T =1650 C) |
|---|---|---|---|---|
| Type K Refractory | 100 | 99.10 | 98.85 | 98.60 |
| Type SiC Refractory | 100 | 98.35 | 97.73 | 97.081 |

Tab. 6 contains the modelling results for the type K refractory when the composition of the Si in the metal was varied and the temperature kept constant at 1600°C. The type K refractory dissolves with increasing concentration of Si, with a maximum of 2.2 g dissolving into the metal. It is interesting to observe that SiC formation occurs due to the reaction between C in the refractory and Si in the metal. A maximum of 3.8 g SiC was formed. Experimental confirmation will be required as to whether the SiC formed remains attached to the refractory wall or dissolves into the SiMn alloy. The former would improve the refractoriness of the type K by the formation of an SiC layer on its wall.

INDEX

***Tab. 6**: Refractory dissolution and SiC formation for the K-type refractory*

| Refractory type | Initial mass (g) | Mass (g) (Si =16%) | Mass (g) (Si=17%) | Mass (g) (Si=18%) |
|---|---|---|---|---|
| Type K Refractory | 100 | 98.63 | 98.21 | 97.78 |
| SiC (formed) | 0 | 0.94 | 2.37 | 3.80 |

Tab. 7 contains the modelling results for the type SiC refractory when the composition of Si in the metal was varied and the temperature kept constant at 1600°C. The type SiC refractory dissolves in the metal with increasing Si composition, up to 17 wt. % Si. A maximum of 1.02 g mass is lost due to dissolution, and this is evident as no products are formed. At an Si composition of 18 wt. %, type SiC refractory has a lower mass loss of 0.46 g .

.

***Tab. 7**: Refractory dissolution and carbon formation for the SiC-type refractory*

| Refractory type | Initial mass (g) | Mass (g) (Si =16%) | Mass (g) (Si=17%) | Mass (g) (Si=18%) |
|---|---|---|---|---|
| C formation | 0 | 0 | 0 | 0 |
| Type SiC Refractory | 100 | 98.40 | 98.98 | 99.54 |

In summary, thermodynamic calculations indicated that:

- Both the type K and type SiC refractory will be subject to wear due to dissolution in the as-received alloy with an increase in temperature. The type K performs better than the type SiC under high temperature conditions of up to 1650 °C.
- Both the type K and type SiC refractory will be subject to wear due to dissolution and chemical reaction with an increase in Si content in the SiMn alloy.
- Operating at a constant temperature of 1600 °C and Si compositions below 16%, the type K will be the better option, whilst at the same operating temperature and higher Si compositions, type SiC will be more suitable.

# CONCLUSION

Industrial SiMn alloy, and two ramming pastes – one carbon-based (type K), the other SiC-based (type SiC)– were sourced, prepared, and characterised. The SiMn alloy sourced for the experimental work is typically a grade C alloy, containing 67.3 wt. % Mn, 1.7 wt. % C, 14.7 wt. % and 16.3 wt. % Fe. The type K refractory contains 86.4 wt. % fixed carbon and 10.9 wt. % ash. The type SiC refractory contains 1.6 wt. % fixed carbon, silicon metal and SiC reported to the ash, with a composition of 95.9 wt. %. The two refractory samples have different physical properties - the type SiC refractory has a higher bulk density and open porosity than the type K refractory. Thermodynamic calculations predicted a dependency of wear of both refractory materials on temperature and silicon-content of the metal. Testing these conditions on laboratory-scale, utilising the rotating finger experimental set-up, will be useful in validating the theoretical results developed here.

INDEX

# REFERENCES


[1] ASTM Standards A483 / A483M - 10, “Standard Specification for Silicomanganese.” ASTM International, West Conshohocken, PA, 2003, pp. 1–2, 2010.

[2] S. E. Olsen, M. Tangstad, and T. Lindstad, *Production of manganese ferroalloys*. Trondheim, Norway: Tapir Academic Press, 2007.

[3] J. D. Steenkamp and J. Basson, “The manganese ferroalloys industry in southern Africa,” *J. South. African Inst. Min. Metall.*, vol. 113, pp. 667–676, 2013.

[4] J. D. Steenkamp, M. Tangstad, P. C. Pistorius, H. Mølnås, and J. Muller, “Corrosion of taphole carbon refractory by CaO-MnO-SiO2-Al2O3-MgO slag from a SiMn production furnace,” in *INFACON XIII*, 2013, pp. 669–676.

[5] J. D. Steenkamp, P. C. Pistorius, and M. Tangstad, “Wear mechanisms of carbon-based refractory materials in silicomanganese tap-holes - Part 1: equilibrium calculations and slag and refractory characterisation,” *Metall. Mater. Trans. B Process Metall. Mater. Process. Sci.*, vol. 46B, no. 2, pp. 653–667, 2015.

[6] J. P. Gous, J. H. Zietsman, J. D. Steenkamp, and J. J. Sutherland, “Excavation of a 48 MVA silicomanganese submerged-arc SiMn furnace in South Africa – Part I: Methodology and Observations,” in *5th International Symposium on High-Temperature Metallurgical Processing*, 2014, pp. 255–269.

[7] J. D. Steenkamp, J. P. Gous, P. C. Pistorius, M. Tangstad, and J. H. Zietsman, “Wear analysis of a taphole from a SiMn production furnace J.,” in *Furnace Tapping Conference 2014*, 2014, pp. 51–64.

[8] J. D. Steenkamp, P. C. Pistorius, and M. Tangstad, “Chemical wear analysis of a tap-hole on a SiMn production furnace,” *J. South. African Inst. Min. Metall.*, vol. 115, no. 3, pp. 199 – 208, 2015.

[9] J. D. Steenkamp, “Chemical Wear of Carbon - Based Refractory Materials In A Silicomanganese Furnace Tap - hole (PhD Thesis),” University of Pretoria, 2014.

[10] J. D. Steenkamp and P. C. Pistorius, “Tap-Hole Wear: Analysis of Daily Average Slag And Metal Compositions of A Single SiMn Smelter,” in *The Fourteenth International Ferroalloys Congress*, 2015, vol. 8, pp. 505–510.

[11] J. D. Steenkamp, P. C. Pistorius, and J. Muller, “Insights into the potential for reduced refractory wear in silicomanganese smelters,” *J. South. African Inst. Min. Metall.*, vol. 116, no. January, pp. 101–108, 2016.

[12] ASTM -A483, “Standard Specification for Silicomanganese,” *Annual Book of ASTM Standards*. ASTM International, West Conshohocken, PA, United States, pp. 1–2, 2010.

[13] “About Elkem Carbon.” .

[14] Elkem Carbon, “Type K Lining Paste, Data Sheet.” Kistiansand, Norway, 2015.

[15] Elkem Carbon, “Elkem Cold Lining Paste Type-SiC, Data Sheet.” Kistiansand, Norway, 2009.

[16] S. Baxendale, “Testing of Refractory Materials,” in *Refractories Handbook*, 2004, pp. 435–474.

[17] ASTM-D3172, “Standard Practice for Proximate Analysis of Coal and Coke 1,” *Annual Book of ASTM Standards*. ASTM International, West Conshohocken, PA, United States, pp. 1–2, 2013.

[18] ASTM-D3174, “Standard Test Method for Ash in the Analysis Sample of Coal and Coke from Coal 1,” *Annual Book of ASTM Standards*. ASTM International, West Conshohocken, PA, United States, pp. 1–6, 2012.

[19] ASTM-D3173, “Standard Test Method for Moisture in the Analysis Sample of Coal and Coke 1,” *Annual Book of ASTM Standards*. ASTM International, West Conshohocken, PA, United States, pp. 1–4, 2011.

[20] SGS, “Proximate and Ultimate Analysis - Mining,” 2015. [Online]. Available: http://www.sgs.co.za/en/Mining/Analytical-Services/Coal-and-Coke/Proximate-and-Ultimate-Analysis.aspx. [Accessed: 01-Jul-2015].

[21] B. Hafner, “Energy Dispersive Spectroscopy On The SEM: A Primer,” *Characterization Facility, University of Minnesota*. pp. 7–10, 2006.

[22] J. H. Chesters, *Refractories Production and Properties*. London, UK: The iron and steel institute, 1963.

[23] M. Mushwana and J. D. Steenkamp, “Apparent Porosity And Bulk Density Measurements of Samples From an Industrial-Scale Söderberg Electrode,” Randburg, South Africa, 2015.

[24] C. Bale, P. Chartrand, S. Degterov, and G. Eriksson, “FactSage thermochemical software and databases,” *Calphad*, vol. 26, pp. 189–228, 2002.

[25] K. Tang and S. E. Olsen, “Computer simulation of equilibrium relations in manganese ferroalloy production,” *Metall. Mater. Trans. B*, vol. 37, pp. 599–606, 2006.


INDEX